Catalysis Science & Technology

Accepted Manuscript

ROYAL SOCIETY OF CHEMISTRY

www.rsc.org/catalysis

Journal Name

RSCPublishing

ARTICLE

Boron Nitride Coated Rhodium Black for Stable Production of Syngas

Cite this: DOI: 10.1039/xoxxoooooox

Andrew C. Chien [†], Jeroen A. van Bokhoven [†,‡,*]

Received ooth January 2012,
Accepted ooth January 2012

DOI: 10.1039/xoxxoooooox

www.rsc.org/

A blanket of hexagonal boron nitride (h-BN) was grown on rhodium black by atmospheric pressure chemical vapor deposition. During methane oxidation at 650 °C the as-synthesized material showed steady syngas production shortly after oxygen interruption, whereas the activity of uncovered rhodium black degraded. The improved activity of the catalyst was attributed to the boron nitride coating, which serves to stabilize rhodium metal and avoid particle agglomeration by carbon deposition. These results present a compelling technique for metal catalyst modification with boron nitride in cases where coking is a problem.

Introduction

Boron nitride is a chemical compound with the chemical formula BN, consisting of equal numbers of boron and nitrogen atoms. BN is isoelectronic with carbon in cubic and hexagonal forms, corresponding to the organization of carbon in diamond and graphite structures, respectively. Analogous to graphite, hexagonal boron nitride (h-BN) displays a layered honeycomb structure comprising alternating boron and nitrogen atoms connected by strong covalent bonds. The strong sp^2 hybridized B-N covalent bonds within h-BN impart high mechanical strength and good chemical stability.[1,2] Significantly, a number of property changes are brought about by the distinctive elemental composition of h-BN, including a large band gap (> 5 eV) and enhanced oxidative resistance.[3] In comparison with graphite, these points of difference make nanostructured h-BN very attractive for application in electronics and may have wider implications in catalysis conducted at high temperatures and under harsh chemical conditions.

Boron nitride has garnered notice in the field of heterogeneous catalysis over the past decade because of excellent thermal and chemical stability.[4–8] Boron nitride supported platinum is an effective catalyst for destruction of volatile organic compounds (VOC) for 80 h with a low light-off temperature (i.e. temperature for 50% conversion). By contrast, platinum supported on alumina deactivates under the same conditions.[9] Additionally, a BN supported barium/ ruthenium catalyst exhibited significant activity and stability during ammonia synthesis at 100 bar and 550 °C over 3500 h.[10] These studies demonstrate promising activity when using BN in a catalyst and show the potential of BN as a support. Interest of incorporating BN in heterogeneous catalysis is growing [11,12] ; this ultimately will increase the need for simple ways of synthesizing novel BN catalysts for future applications.

Synthesis of h-BN on transition metals has become important as BN demonstrates potential as a template for nano-device fabrication[13,14] and for immobilization of molecules.[15,16] One and few layers of h-BN are successfully obtained in ultrahigh vacuum on single crystals by chemical vapor deposition (CVD). Decomposition of precursor molecules, such as borazine ($B_3N_3H_6$), on a hot metallic surface in CVD leads to spontaneous formation of a regular hexagonal monolayer. [17] These attempts are followed by atmospheric pressure chemical vapor deposition (APCVD) on polycrystalline metals for controllable multi-layer growth.[18,19] While two-dimensional planar substrates are widely adopted in these studies, no information pertaining to substrates of irregular shapes is reported. Early investigations on powdered substrate focus on transition metal oxides, such as magnesium oxides [20], silver oxides [21], iron oxides (α-Fe_2O_3) [22,23], and aluminum oxides [24]. None of these materials are used as catalysts.

Oxidation of methane to synthesis gas is of continuing interest for conversion of natural gas into hydrogen and valuable chemicals.[25–28] While noble metals such as platinum and rhodium present excellent catalytic properties, metal agglomeration and carbon deposition cause partially irreversible deactivation. Herein we demonstrate a method for synthesis of h-BN on polycrystalline rhodium black by APCVD and subsequent application of these materials in methane oxidation. This facile and rational method uses rhodium black as a model for post-synthetic treatment, circumventing agglomeration and particle growth usually associated with deactivation of nano-sized metal catalysts. The use of BN to actively promote and stabilize metal catalysts, rather than as a mere passive support, remains unexplored. In this study, the synthesis, catalytic activity, and factors affecting the reaction activity of BN-rhodium metal catalyst are presented. Our results reveal scope for improvement of heterogeneous catalyst performance and stability using BN coated metals - findings which will ultimately contribute to development of a new generation of stable, highly active, and selective catalysts.

Experimental Section

Synthesis of Boron Nitride on Rhodium

Figure 1 illustrates the experimental setup for synthesis of boron nitride. Boron nitride was grown on rhodium black (American element) by CVD using borazine as a precursor. Borazine was obtained according to literature [29,30] from ammonium sulfate and sodium borohydride in tetraglyme at 120-140 °C. Prior to CVD, two grams of rhodium particles capped with quartz wool were placed in a quartz tube and heated under a flow of helium to 800 °C. The CVD was then conducted at 800 °C under ambient pressure by switching the gas flow from the bypass position to the saturator, thus allowing borazine to decompose on hot rhodium. The decomposition of borazine occurred via dehydrogenation, which was monitored by hydrogen production and borazine concentration in an effluent stream by an on-line mass spectrometer (MS; GSD 300 O_2, Pfeiffer Vacuum OmniStar). The MS inlet allowed a portion of the atmospheric pressure effluent to enter an ionization chamber at approximately 0.7 mbar. The mass/electron ratios (m/e) were selected for H_2 (2), He (4), boron (11), N_2 (28), and borazine (80). After CVD, the gas flow was switched back to bypass, followed by annealing of the borazine-deposited material at 950 °C for 1 h. Thereafter, the sample was cooled down to room temperature and ground to a fine powder for subsequent characterization and reaction.

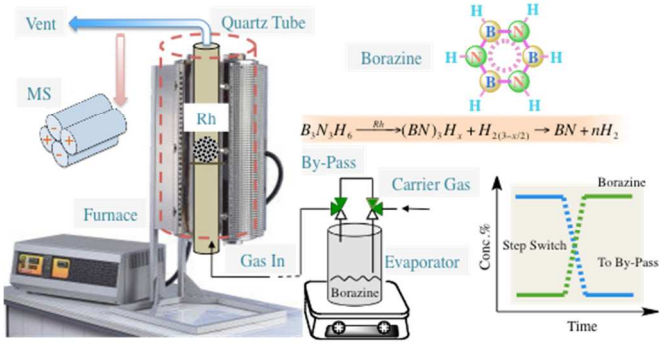

Fig. 1 APCVD set-up for boron nitride synthesis on rhodium black

Methane Oxidation Reaction

Methane oxidation and temperature-programmed oxidation were investigated using a CATLAB system (Hiden Analytical) equipped with a plug-flow reactor and an integrated mass spectrometer. Rhodium black or the as-synthesized BN-Rh about 50 mg was loaded into a quartz tube in CATLAB and heated to reaction temperature with a mixture of methane and oxygen (mole ratio: CH_4/O_2 = 2) in a helium stream. Specific flow rates are denoted in figure captions in results section. Composition of the reaction effluents was continuously monitored by mass spectrometry. Conversion of methane (based on methane concentration) and selectivity of products are calculated by calibrated MS intensity of gas species, i.e. partial pressure. The mass/ electron ratios (m/e) in MS were selected for H_2 (2), He (4), CH_4 (15), H_2O (18), CO (28), O_2 (32), and CO_2 (44). The intensity for H_2 (2) and CO (28) were calibrated by further subtracting their contributions from the CH_4 and CO_2 signals, respectively.

Characterization of As-Synthesized Material

The morphology of the as-synthesized BN-Rh material was characterized by scanning electron microscope (SEM; ZEISS Ultra 55) and transmission electron microscope (TEM; Hitachi). Elemental composition was determined by an energy-dispersive X-ray spectrometer (EDX) and X-ray photoelectron spectroscopy (XPS). X-ray photoelectron spectroscopy (XPS) was conducted using a VG ESCALAB 220iXL spectrometer (Thermo Fisher Scientific) with a focused Al Kα mono-source (spot size: 500 µm, power: 150 Watt) and a magnetic lens system.

Results

Figure 2 presents MS profiles monitoring elution of precursors and resultant gas products during the synthesis of boron nitride. The MS profiles of effluent gas species reveal a peak in hydrogen production proceeded by borazine while borazine concentration oscillates, after gas switching from bypass to a borazine saturator. Both hydrogen and borazine concentration reached steady state in a short period. Repeating the gas-switch step confirmed that the concentration of eluting hydrogen and borazine is stable. Annealing to higher temperature (i.e. from 800 to 950 °C) caused further dehydrogenation and generation of boron nitride. Electron micrographs in Figure 3 display the morphology of the as-synthesized boron nitride layer on rhodium. SEM (Fig. 3a) clearly indicates formation of a coating on top of pristine rhodium black after CVD. The thickness of the coating approaches 50 nm in TEM micrographs (Fig. 3b). Magnification at a scale of 5 nm indicates that the coating consists of multiple layers separated by approximately 0.35 nm, corresponding to hexagonal boron nitride (h-BN).

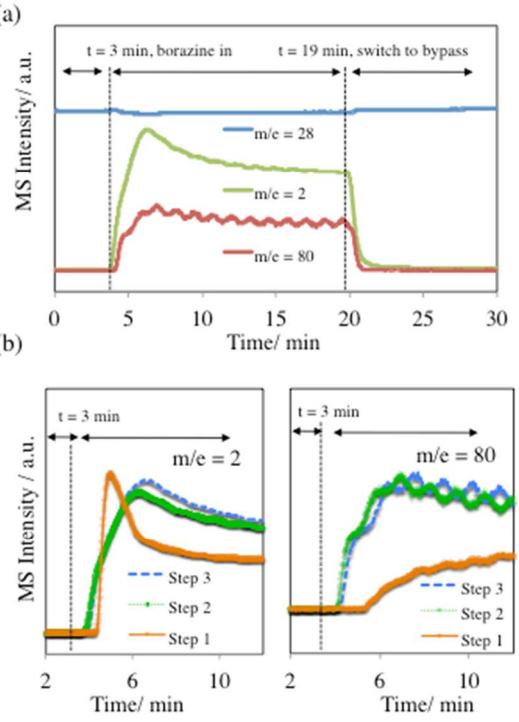

Fig. 2 (a) MS profiles of effluent species and (b) repeated steps during CVD of borazine on rhodium black at 800 °C

The elemental composition of boron nitride coated rhodium was further characterized by energy dispersive X-ray spectroscopy (EDX) in Figure 4. EDX identifies rhodium and an additional nitrogen component on the as-synthesized material, while boron could not be detected because of experimental limitations. X-ray photoelectron spectroscopy (XPS) confirmed presence of both boron and nitrogen on the as-synthesized sample (Fig. 4b). As a result of

boron-nitride shielding, the rhodium signal on the synthesized catalyst presents a suppressed XPS intensity.

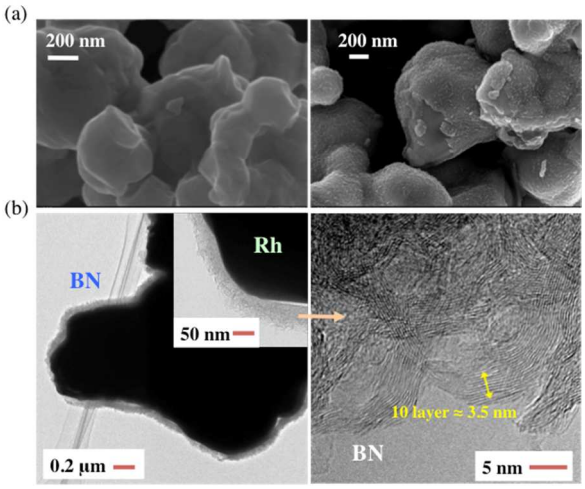

Fig. 3 Electron micrographs of boron nitride coating on rhodium, (a) SEM images of rhodium particles before (left) and after (right) CVD; (b) TEM image displaying layer thickness and morphologies of boron nitride in the magnified inset

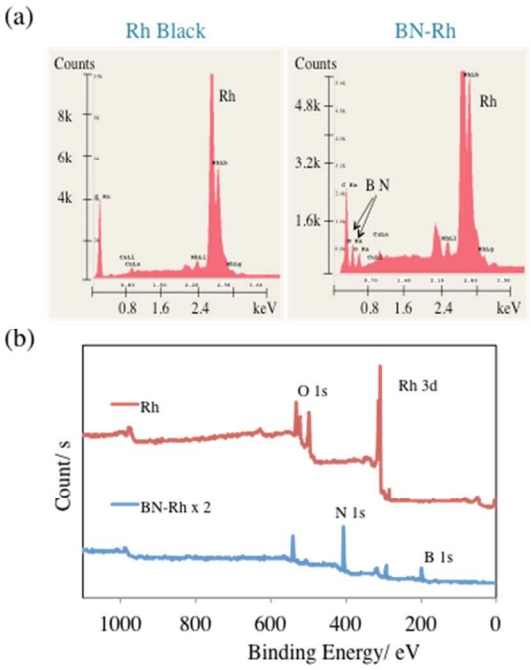

Fig. 4 (a) EDX spectra of rhodium black before (left) and after (right) CVD; (b) XPS spectra on these two samples (XPS intensity multiplied by two in BN-Rh)

Figure 5 shows that the boron nitride coated rhodium catalyst enhances syngas production in methane oxidation after interrupting oxygen for 30 min. Prior to the interruption, the catalyst displayed almost no activity at 650 °C. Cessation of the oxygen flow induced production of hydrogen and carbon monoxide, trending downward over time. Resuming the oxygen flow caused a drastic increase of syngas production, which proceeded in a stable fashion for days. Non-boron nitride coated rhodium black show no such enhancement and the activity decreased due to agglomeration of metal particles (Figure 6). The conversion and product selectivity on methane oxidation for both catalysts is shown on Table 1 for comparison. Examination of the boron nitride coated rhodium by TEM after the reaction indicates peeling of the boron-nitride layer away from the rhodium surface, leaving the metal partially exposed. TEM (Figure 7) identifies a distinct phase entirely different from the original boron nitride on rhodium. In contrast to the freshly prepared lax structure of boron nitride, the new phase adheres well to the substrate and exhibits dense packing of multi-layers with inter-layer distances of about 3.5 Å. Oxidation seems to remove this new phase, which is a carbon-containing species adsorbed on the spent catalyst according to temperature-programmed oxidation experiments (TPO) (Figure 8).

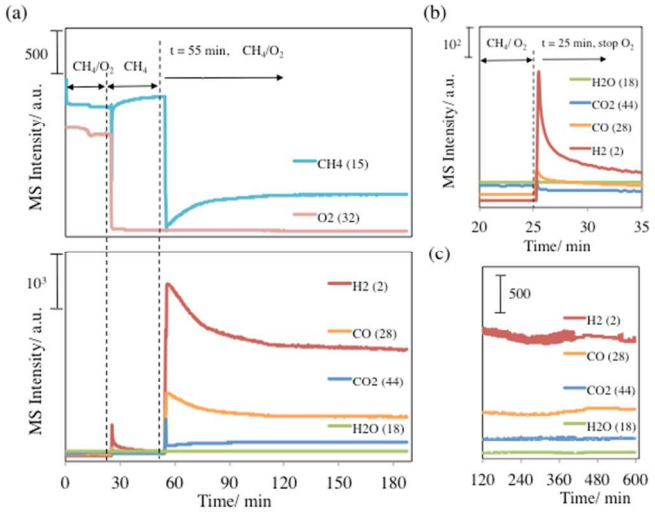

Fig. 5 (a) MS profiles of gas species eluting during methane oxidation over boron nitride coated rhodium at 650 °C, after (b) 20-45 min, and (c) 120-600 min; 5% CH_4/He (80 sccm) and O_2 (2 sccm)

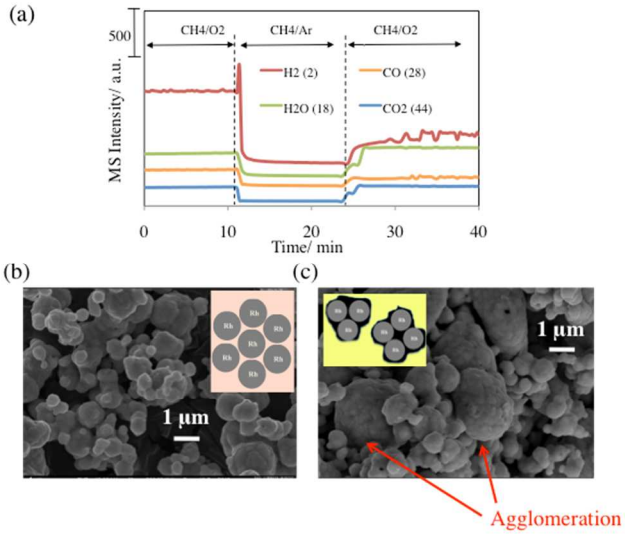

Fig. 6 (a) MS profiles of Rh black degradation during methane oxidation, and SEM images of rhodium metal particles before (b) and after (c) the reaction; CH_4 flow rate 80 sccm (5% methane in helium) and pure O_2 2 sccm at 650 °C

Tab. 1 Conversion and selectivity of Rh and BN-Rh catalysts on methane oxidation

	T / °C	Conversion / %		Selectivity/ %				
		CH_4	O_2	H_2	H_2O	CO	CO_2	total
Rh	450	33.6	96.1	14.1	50.0	5.0	30.9	100.0
	550	33.8	97.6	27.8	38.2	8.8	25.2	100.0
	650	50.7	98.2	50.4	18.3	18.4	12.9	100.0
BN-Rh	450	0	0	--	--	--	--	--
	550	3.4	4.5	24.4	42.2	14.9	18.5	100.0
	650	6.8	12.5	10.3	53.7	8.0	28.0	100.0
	650*	78.5	97.9	60.6	7.2	25.0	7.2	100.0

* : Valued obtained after interruption of oxygen flow
Note: Conversion of methane and oxygen is based on $[(C_{in}-C_{out})/ C_{in}] \times 100\%$ with~ 60 mg catalyst. The error % is ~ ±5%

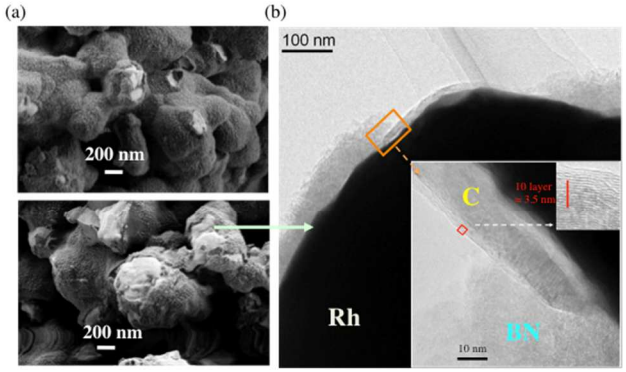

Fig. 7 SEM images of as-synthesized boron nitride coated rhodium before (top) and after (bottom) methane oxidation; (b) TEM images of a distinct phase appearing after methane oxidation

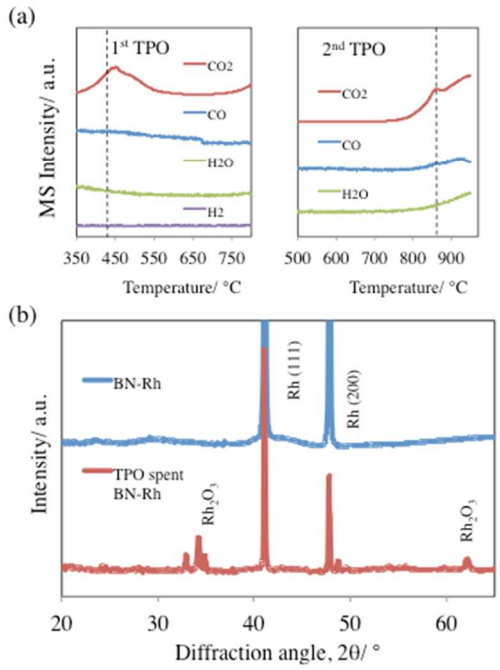

Fig. 8 (a)Temperature-programmed oxidation of spent BN-Rh after methane oxidation (note: 2nd TPO was repeated after first one on the same sample), and (b) X-ray diffraction pattern of spent BN-Rh and the resultant sample after TPO

Discussion

Synthesis of Boron Nitride on Rhodium

A thin layer of hexagonal boron nitride is deposited on rhodium black using an APCVD technique involving decomposition of borazine. Evolution of hydrogen and oscillation of borazine concentration in Fig. 2 indicate that decomposition of borazine is taking place on rhodium surface via dehydrogenation:

$$H_6B_3N_3 \rightarrow (BN)H_x + H_{2(3-x/2)} \rightarrow BN + yH_2$$

When borazine decomposes, its concentration decreases with downward MS intensity. As BN forms and covers active sites, the rate of decomposition slows down, therefore MS intensity of borazine increasing again and giving rise to oscillating pattern. Boron nitride forms a single nano-mesh layer on Rh, Ni, Ru, and Pt single crystals.[17–19] A second layer grows very slowly and requires a much higher amount of precursor. [31] The type of multi-layer growth observed in this study is also reported on polycrystalline transition metal foils or films prepared by APCVD at lower temperatures. The apparent difference in mechanism and kinetics of layer growth appears to arise due to variations in the type of material or the pressure/ temperature parameters used. In accordance with previous studies, the polycrystalline nature and ambient pressure CVD conditions described in the current system favor multilayer growth. [17–19] In addition to this interesting layer thickness phenomenon, we also observe that rhodium is not enclosed by boron nitride but instead presents a partially exposed surface. Loose bonding of boron nitride and metal could be attributed to a lattice mismatch between the two entities. Strong lattice mismatch of hexagonal boron nitride on Rh (111) has been demonstrated with a single boron nitride layer, which favored bonding interactions in only some areas of the (13 x 13) unit cell, while in other areas interactions were repelled by the surface due to strong cohesive forces within the layer. [32] Multiple layers of boron nitride are known to maintain loose bonding between the metal surface and boron nitride. The lattice mismatch between boron nitride and transition metal is much smaller for Ni (111),[33] which is consistent with our studies on nickel metallic powder where boron nitride is well adhered.

Catalysis of Boron Nitride Covered Rhodium

During methane oxidation, the boron-nitride coated rhodium shows enhanced and stable syngas production at 650 °C only after interruption of the oxygen flow. The activity of the catalyst remains low prior to oxygen cessation. SEM images suggest that bare metal becomes exposed after methane flushing. The BN itself is inert in catalytic reactions while the corrugate structure of BN blanket on rhodium is not. The peeling of BN layer could be resulted from loosely bonded multilayer structure and incomplete enclosure due to lattice mismatch between BN and metal substrate. The uncovered rhodium thus serves as an active site for methane dissociation while the remaining boron nitride prevents metal sintering. On the other hand, TEM images reveal that a graphite-like structure forms after the reaction in proximity to boron nitride, possibly due to methane pyrolysis. The presence of carbon is further evidenced by temperature-programmed oxidation of the spent catalyst, which expelled carbon dioxide as a major product at 450 °C and above 800 °C (Fig. 8). Evolution of carbon dioxide at different temperatures infers that carbon exists in different forms with varying bonding

strength on the surface. After the TPO studies, rhodium is partially oxidized to rhodium oxide and no graphite structure is observed. This carbon layer does not prevent the catalytic reaction from occurring.

A mechanism for enhanced syngas production on the boron nitride coated rhodium is proposed in Figure 9. Upon interruption of oxygen flow at elevated temperature surface oxides on the exposed metal convert to reduced active sites [34,35], thus allowing methane dissociation to C_{ad} and H_{ad} (adsorbed species). The adsorbed hydrogen (H_{ad}) combines and desorbs as H_2. The adsorbed carbon (C_{ad}) forms graphite and eventually spalls up the boron nitride (i-ii). As methane dissociates carbon accumulates and occupies the active site on the metal surface (ii-iii), leading in turn to retarded dissociation of methane and decreasing H_2 production. H_2 production increases once again when an oxygen flow is resumed. Oxygen refreshes active sites by oxidatively removing carbon, thus regenerating a reduced surface from which methane may readily dissociate to produce syngas.

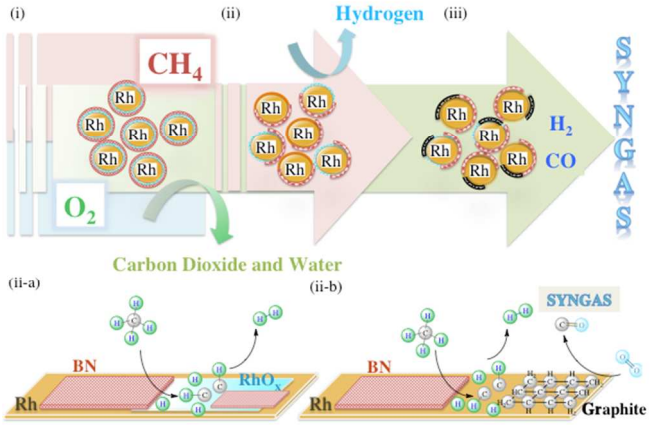

Fig. 9 Proposed mechanism for syngas production on boron nitride covered rhodium, i) inactive boron-nitride site or surface oxide for production of carbon dioxide and water, ii) reduction of surface oxides in the absence of oxygen (ii-a) and spalling-up of boron nitride due to carbon formation (ii-b; beginning of iii with a resumed oxygen flow) , and iii) enhanced syngas production on exposed rhodium sites stabilized by residual boron nitride

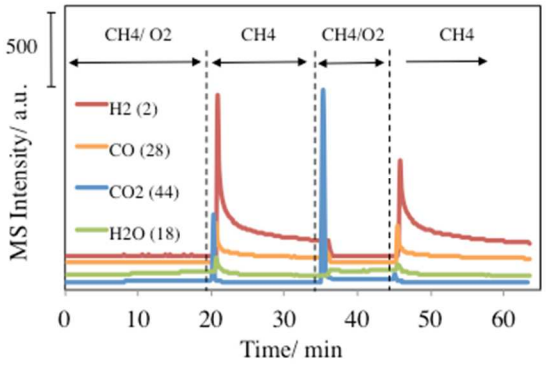

Fig. 10 MS profiles of gas species formed during methane oxidation on boron doped rhodium black (50mg) at 650 °C in 5% CH_4/ He 80 sccm and O_2 2 sccm

We ascribe the stable operation of our BN-rhodium metal catalyst to the avoidance of particle agglomeration and loss of active sites from carbon deposition. The effect of BN on improved stability and catalytic performance was regarded as "structural promotion". BN serves as a barrier layer to prevent coking and stabilize metal. This barrier-stabilizing concept has received significant attention recently, such as coating or encapsulation of noble metal with an oxide layer of alumina [36] and silica [37]. In terms of boron or nitride, none has been reported yet. On the other hand, Xu et. al.[38] report that 1 wt.% boron effectively promotes nickel catalysts in methane steam reforming and prevents coking. Successful promotion is attributed to occupation of step and sub-surface octahedral sites by boron, thus preventing carbon from diffusion into the bulk metal. In the boron nitride covered rhodium nanoparticles, occupation of sub-surface sites by boron nitride seems unlikely due to the large molecular size of this structure; blocking on step sites is more plausible. If this is the case, partial covering of rhodium with boron nitride is probably sufficient to accomplish catalytic promotion, whereas complete enclosure of boron nitride on rhodium is unnecessary. To clarify the role of boron versus boron nitride in catalytic promotion we prepared a 2 wt. % boron doped rhodium material for application in methane oxidation. Addition of boron kills the activity of rhodium and no syngas production was observed (Figure 10). A similar catalytic inactivity is witnessed in the case of a benzene-pyrolyzed rhodium and material derived from unsuccessful boron-nitride synthesis on rhodium (boron species appear on the surface). Since both boron and carbon are predisposed towards adsorption on rhodium we may deduce that catalytic activity is probably lost as a result of blocking of the active sites.

Conclusions

A blanket of boron nitride can be grown on rhodium black by an APCVD technique. Unlike uncovered rhodium, the boron-nitride coated rhodium consistently catalyzed syngas production by methane oxidation after interruption of oxygen gas flow. We have determined that coating of metal particles with a non-continuous layer of boron nitride prevents loss of active site from coking and promotes stable catalyst operation. Our novel BN-rhodium catalyst expands on the existing potential of transition metal catalysts by using boron nitride to subtly modify the characteristics and behavior of the metal surface. The techniques reported herein may find applicability in other catalytic applications.

Acknowledgements

This work was supported by Paul Scherrer Institute, Switzerland. The authors would like to acknowledge Professor Jürg Osterwalder for discussion, Frank Krumeich and Erick De Boni for STEM imaging, Mario El Kazzi for XPS analysis, Thanh-Bin Troung for borazine synthesis, and Kim Meyer for proof reading.

† Paul Scherrer Institute, 5232 Villigen PSI, Switzerland
‡ ETH Zürich, Institute for Chemical and Bioengineering, 8093 Zürich, Switzerland
* Corresponding author: jeroen.vanbokhoven@chem.ethz.ch

References

1 T. Oku, I. Narita, N. Koi, A. Nishiwaki, M. Inoue, K. Hiraga, T. Matsuda, H. Tokoro, S. Fujii, M. Gonda, T. Hirai, R. V

Belosludov and Y. Kawazoe, *B-C-N Nanotubes and Related Nanostructures*, Springer New York, New York, NY, 2009.
2 A. Pakdel, C. Zhi, Y. Bando and D. Golberg, *Mater. Today*, 2012, **15**, 256–265.
3 Z. Liu, Y. Gong, W. Zhou, L. Ma, J. Yu, J. C. Idrobo, J. Jung, A. H. MacDonald, R. Vajtai, J. Lou and P. M. Ajayan, *Nat. Commun.*, 2013, **4**, 2541.
4 G. Postole, A. Gervasini, C. Guimon, A. Auroux and B. Bonnetot, *J. Phys. Chem. B*, 2006, **110**, 12572–12580.
5 G. Postole, M. Caldararu, B. Bonnetot and a. Auroux, *J. Phys. Chem. C*, 2008, **112**, 11385–11393.
6 J. C. S. Wu and H.-C. Chou, *Chem. Eng. J.*, 2009, **148**, 539–545.
7 C. Jacobsen, *J. Catal.*, 2001, **200**, 1–3.
8 S. H. Taylor and A. J. J. Pollard, *Catal. Today*, 2003, **81**, 179–188.
9 J. C.-S. Wu, Z.-A. Lin, J.-W. Pan and M.-H. Rei, *Appl. Catal. A Gen.*, 2001, **219**, 117–124.
10 T. W. Hansen, J. B. Wagner, P. L. Hansen, S. Dahl, H. Topsøe and C. J. Jacobsen, *Science*, 2001, **294**, 1508–1510.
11 A. Lyalin, A. Nakayama, K. Uosaki and T. Taketsugu, *J. Phys. Chem. C*, 2013, **117**, 21359–21370.
12 S. Lin, X. Ye, R. S. Johnson and H. Guo, *J. Phys. Chem. C*, 2013, **117**, 17319–17326.
13 Y. Shi, C. Hamsen, X. Jia, K. K. Kim, A. Reina, M. Hofmann, A. L. Hsu, K. Zhang, H. Li, Z. Juang, M. S. Dresselhaus, L. Li and J. Kong, *Nano Lett.*, 2010, **10**, 4134–4139.
14 R. Y. Tay, M. H. Griep, G. Mallick, S. H. Tsang, R. S. Singh, T. Tumlin, E. H. T. Teo and S. P. Karna, *Nano Lett.*, 2014, **14**, 839–46.
15 H. Cun, M. Iannuzzi, A. Hemmi, S. Roth, J. Osterwalder and T. Greber, *Nano Lett.*, 2013, **13**, 2098–2103.
16 H. Dil, J. Lobo-Checa, R. Laskowski, P. Blaha, S. Berner, J. Osterwalder and T. Greber, *Science*, 2008, **319**, 1824–1826.
17 M. Corso, W. Auwärter, M. Muntwiler, A. Tamai, T. Greber and J. Osterwalder, *Science*, 2004, **303**, 217–220.
18 Y. Gao, W. Ren, T. Ma, Z. Liu, Y. Zhang, W. Liu and L. Ma, *ACS Nano*, 2013, **7**, 5199–5206.
19 G. Kim, A.-R. Jang, H. Y. Jeong, Z. Lee, D. J. Kang and H. S. Shin, *Nano Lett.*, 2013, **13**, 1834–9.
20 R. T. Paine and C. K. Narula, *Chem. Mater.*, 1989, **1**, 486–489.
21 T. Oku, T. Kusunose, K. Niihara and K. Suganuma, *J. Mater. Chem.*, 2000, **10**, 255–257.
22 H. T. Ã, S. Fujii, T. Oku, T. Segi and S. Nasu, *Mater. Trans.*, 2004, **45**, 2941–2944.
23 H. Tokoro, S. Fujii and T. Oku, *Solid State Commun.*, 2005, **133**, 681–685.
24 S. K. Klitgaard, K. Egeblad, M. Brorson, K. Herbst and C. H. Christensen, *Eur. J. Inorg. Chem.*, 2007, **2007**, 4873–4876.
25 B. Christian Enger, R. Lødeng and A. Holmen, *Appl. Catal. A Gen.*, 2008, **346**, 1–27.
26 S. a. Al-Sayari, *Open Catal. J.*, 2013, **6**, 17–28.
27 S. S. Bharadwaj and L. D. Schmidt, *Fuel Process. Technol.*, 1995, **42**, 109–127.
28 R. Frind, L. Borchardt, E. Kockrick, L. Mammitzsch, U. Petasch, M. Herrmann and S. Kaskel, *Catal. Sci. Technol.*, 2012, **2**, 139–146.
29 E. E. R. Thomas Wideman, Paul J. Fazen, Anne T. Lynch, Kai Su and L. G. Sneddon, *39. borazine, polyborazylene, b-vinylborazine, and poly(b-vinylborazine)**, John Wiely & Sons, Inc., 1998, vol. 32.
30 J. Li, C. Zhang, B. Li, F. Cao and S. Wang, *Eur. J. Inorg. Chem.*, 2010, **5**, 1763–1766.
31 A. Nagashima and N. Tejima, *Phys. Rev. B*, 1995, **51**, 4606–4613.
32 J. Gómez Díaz, Y. Ding, R. Koitz, A. P. Seitsonen, M. Iannuzzi and J. Hutter, *Theor. Chem. Acc.*, 2013, **132**, 1350–1366.
33 W. Auwärter, T. J. Kreutz, T. Greber and J. Osterwalder, *Surf. Sci.*, 1999, **429**, 229–236.
34 R. Singh and S. Chuang, *Catal. Commun.*, 2008, **9**, 1235–1242.
35 S. Fouladvand, *Catal. Sci. Technol.*, 2014, **4**, 3463–3473.
36 J. Lu, J. W. Elam and P. C. Stair, *Acc. Chem. Res.*, 2013, **46**, 1806–1815.
37 Y. Dai, B. Lim, Y. Yang, C. M. Cobley, W. Li, E. C. Cho, B. Grayson, P. T. Fanson, C. T. Campbell, Y. Sun and Y. Xia, *Angew. Chem. Int. Ed. Engl.*, 2010, **49**, 8165–8168.
38 J. Xu, L. Chen, K. Tan, a Borgna and M. Saeys, *J. Catal.*, 2009, **261**, 158–165.

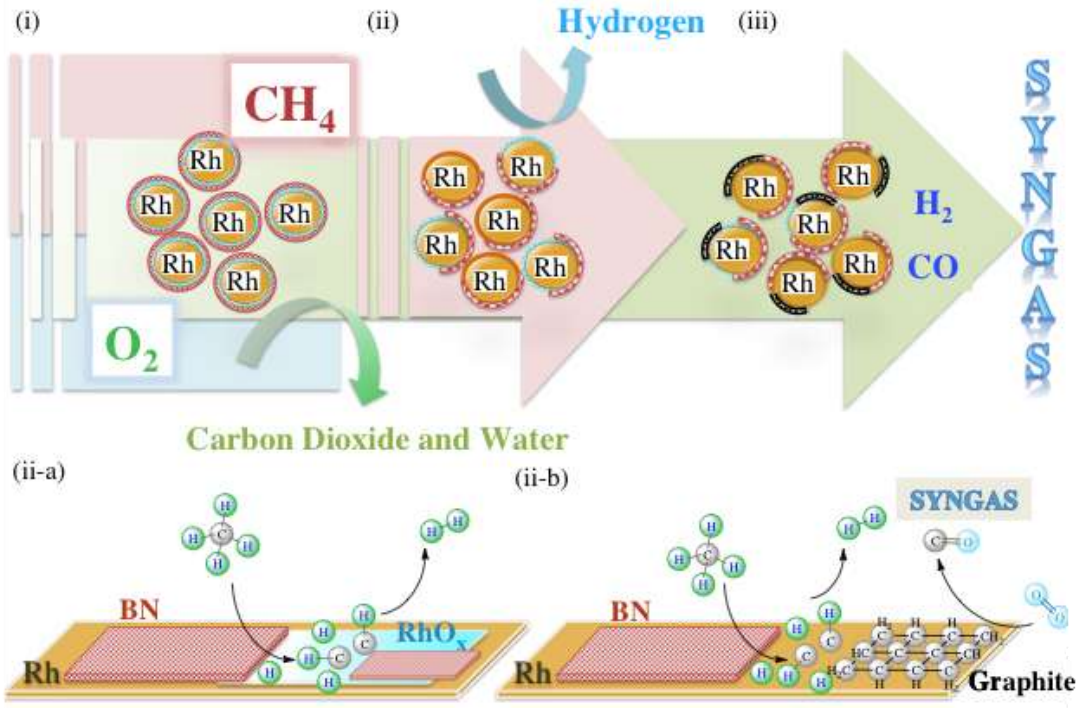

- A blanket of boron nitride grown by CVD stablizes Rhodium black for syngas production in methane oxidation and avoid agglomeration of metal particle by carbon deposition.